sustainability

MDPI

Article

Technical Performance Prediction and Employment Potential of Solar PV Systems in Cold Countries

Ephraim Bonah Agyekum [1,*], Usman Mehmood [2,3], Salah Kamel [4], Mokhtar Shouran [5], Elmazeg Elgamli [5,*] and Tomiwa Sunday Adebayo [6,7]

1 Department of Nuclear and Renewable Energy, Ural Federal University Named after the First President of Russia Boris Yeltsin, 19 Mira Street, 620002 Ekaterinburg, Russia
2 Remote Sensing, GIS and Climatic Research Lab, National Center of GIS and Space Applications, Centre for Remote Sensing, University of the Punjab, Lahore 54590, Pakistan; usmanmehmood.umt@gmail.com
3 Department of Political Science, University of Management and Technology, Lahore 54770, Pakistan
4 Electrical Engineering Department, Faculty of Engineering, Aswan University, Aswan 81542, Egypt; skamel@aswu.edu.eg
5 Wolfson Centre for Magnetics, School of Engineering, Cardiff University, Cardiff CF24 3AA, UK; shouranma@cardiff.ac.uk
6 Department of Business Administration, Faculty of Economics and Administrative Science, Cyprus International University, Nicosia 99040, Turkey; twaikline@gmail.com
7 Department of Finance & Accounting, AKFA University, Tashkent 100012, Uzbekistan
* Correspondence: agyekumephraim@yahoo.com (E.B.A.); elgamlies@cardiff.ac.uk (E.E.)

Abstract: Power distribution to decentralized and remote communities secluded from centralized grid connections has always been a problem for utilities and governments worldwide. This situation is even more critical for the isolated communities in Russia due to the vast nature of the country. Therefore, the Russian government is formulating and implementing several strategies to develop its renewable energy sector. However, very little information is available on the possible performance of solar photovoltaic (PV) modules under Russian weather conditions for all year round. Thus, this study has been designed to fill that research gap by assessing the performance ratio (*PR*), degradation, energy loss prediction, and employment potential of PV modules in the Sverdlovsk region of Russia using the PVsyst simulation model. A side-by-side comparison of the fixed tilted plane and tracking horizontal axis East–West were analyzed. According to the results, the annual production probability (P) for the fixed PV module for a P50, P75, and P90 is 39.68 MWh, 37.72 MWh, and 35.94 MWh, respectively, with a variability of 2.91 MWh. In the case of the tracking PV module, the annual production probability for the P50, P75, and P90 is 43.18 MWh, 41.05 MWh, and 39.12 MWh, respectively, with a variability of 3.17 MWh. A *PR* of 82.3% and 82.6% is obtained for the fixed and tracking systems, respectively, while the PV array losses for the fixed and tracking orientations are 15.1% and 14.9%, respectively. The months of May to August recorded the highest array losses due to the high temperatures that are usually recorded within that period.

Keywords: renewable energy; solar photovoltaic energy; degradation rate; PVsyst software; energy loss prediction

Citation: Agyekum, E.B.; Mehmood, U.; Kamel, S.; Shouran, M.; Elgamli, E.; Adebayo, T.S. Technical Performance Prediction and Employment Potential of Solar PV Systems in Cold Countries. *Sustainability* **2022**, *14*, 3546. https://doi.org/10.3390/su14063546

Academic Editors: Nicu Bizon, Bhargav Appasani and Mamadou Baïlo Camara

Received: 11 February 2022
Accepted: 12 March 2022
Published: 17 March 2022

1. Introduction

One challenge confronting the world today is how to generate energy in a more sustainable way to meet its energy needs while maintaining environmental security. The world's demand for electricity is growing due to increasing global population, improved lifestyle, and industrialization [1]. It has been estimated that fossil fuel forms about 80% of the world's primary energy, and energy consumption globally is expected to increase by 2.3% each year from 2015 to 2040 [2]. The concentration of atmospheric carbon dioxide (CO_2) equivalent is said to have almost doubled since the inception of the Industrial

Revolution [3]. This has increased the average global temperature, which is negatively impacting global climate [4,5].

Solar photovoltaic (PV) technology can generate power by directly converting incident solar radiation to electrical power [6,7]. PV technology is one of the renewable energy (RE) options that can help to decarbonize the world to decrease greenhouse gas (GHG) emissions. The continual drop in the cost of PV systems and the formulation of policies by various governments to promote the development and use of RE technologies has led to the rapid growth of the PV industry [8]. The PV industry has witnessed a composite yearly growth rate of more than 40% during the last 15 years, making it one of the fast-growing industries globally. This has necessitated the need to improve project designs and continuous monitoring and prediction of the performance of the PV systems that have either been installed or yet to be installed to ensure their reliability and performance [8].

Therefore, several researchers have performed studies that either assess the performance of already installed or yet to be installed PV power plants in several countries. Malvoni et al. [8] examined a 960 kWp monocrystalline silicon PV system's performance in southern Italy. They obtained a capacity factor (*CF*) and performance ratio (*PR*) of 15.6% and 84.4%, respectively. Kumar et al. [9] studied the performance, degradation, and energy loss of a 200 kW roof-integrated crystalline PV system in northern India. According to their results, the PV system is projected to operate with an annual *PR*, *CF*, and energy loss of 77.27%, 16.72%, and −26.5%, respectively. Ramanan et al. [10] evaluated the performance of two colocated grid-connected PV power plants, which consist of copper indium selenium (CIS) and polycrystalline silicon (p-Si) arrays. A yearly *PR* of 86.73% for the CIS and 78.48% for p-Si were obtained, while the capacity utilization factor ranges from 17.99% for the p-Si to 19.57% for the CIS systems. Similarly, Ameur et al. [11] analyzed and compared several indices that affect the performance of different grid-connected PV technologies, i.e., polycrystalline silicon (pc-Si), amorphous silicon (a-Si), and monocrystalline silicon (mc-Si) with capacities of 2 kWp each. The study's outcome suggests that the polycrystalline, monocrystalline, and amorphous technologies generated a four-year yearly alternating current (*AC*) energy average of 3239 kWh, 3246 kWh, and 2797 kWh with yearly *PR* of 77%, 77%, and 73%, respectively. Dahmoun et al. [12] explored and assessed the performance of a 23.92 MWp polycrystalline PV power plant located in El Bayadh in Algeria. Their study shows that the degradation of the *PR* during the study period is estimated to be 0.76% per year.

Furthermore, Kittner et al. [13] evaluated the economic investment, embodied energy, and CO_2 payback for amorphous silicon thin film and single crystalline systems. They reported that the amorphous silicon thin-film panels have higher net environmental and economic benefits. Padmavathi and Daniel [14] worked on a 3 MW grid-connected polycrystalline PV power plant in India. They evaluated normalized technical performance parameters for the system for the year 2011. The generated yearly average energy by the plant was 1372 kWh per kWp. Radue and van Dyk [15] reported losses of up to 30% for thin-film PV power plants sited in South Africa after a period of 14 months. Kymakis et al. [16] also estimated the performance of a 171 kWp polycrystalline silicon PV power plant installed on the island of Crete. After one year, the average annual *PR* and *CF* were 67.36% and 15.26%, respectively. Belmahdi and El Bouardi [17] evaluated the performance of a 1 MW solar PV power plant under Moroccan weather conditions using the PVsyst software. The optimal angle for the installation of the PV module for the study area in summer was identified to be 32° for fixed tilt and 48° for winter on seasonal adjustment tilts. A 60 kWp PV module was modelled for the Uttar-Pradesh area in India using the PVsyst software by [18]. Their system generated a total of 89.5 MWh per year with a performance ratio of 73.73%. In the Philippines, Dellosa et al. [19] assessed the technical and economic performance of 5 MWp PV system for that country using the PVsyst software. The results from their study revealed that the temperature of the PV panel accounted for the highest energy loss; it accounted for 8% of the loss. A payback period of 4.23 years was recorded for the system.

Finally, Chabachi et al. [20] assessed the performance of a poly-Si/6 MWp in Southwest Algeria. An average monthly efficiency for their PV array was 12.68% with a *PR* of 84%. Yadav et al. [21] employed the PVsyst software to examine the performance of a 295 Wp Si-poly PV module SYP295S under Nepal's weather conditions at Tribhuvan University. Their simulation results revealed that a total of 110 kWp of PV power plant's output would be enough for the whole campus. The designed system produced a surplus energy of 115.1 MWh/year, which can be exported to grid. A 2.4 kWp monocrystalline PV module was studied by [22] at the Mulhouse campus, France. The studied power plant generated a total of 5597.65 kWh of energy. Chandel and Chandel [23] conducted a performance assessment on a 19-MWp (17-MWac) PV plant installed with seasonal adjustable tilt (AT), fixed tilt (FT), and horizontal single-axis solar tracking (HSAT) configurations in India. Key findings from their study suggest that the studied FT system recorded an annual *PR* of 79% with a *CF* of 19%. The AT also recorded a *CF* of 20%, while the HSAT recorded 22%. Kumar et al. [24] also assessed a 10 kWp poly-Si PV power plant for the remote islands of Andaman and Nicobar in India. A yearly average *CF* and *PR* range of (13.73–14.61%) and (64.70–64.93%), respectively were obtained. Other studies, such as [25–27] investigated power plants with capacities ranging from 1.72–5 kWp and determined their performance parameters.

RE development and application in the Russian Federation are relatively lower than in other European countries. The country has mainly relied on fossil fuels and nuclear energy for its electricity and heating demands. Hydropower constitutes a large portion of its installed RE capacity in terms of renewables. The country's total installed RE capacity increased to 53.5 GW; hydro alone constitutes 51.5 GW, with bioenergy taking only 1.35 GW. The solar PV has only 460 MW, while onshore wind also has 111 MW as of 2015 [28]. The country's share of installed solar and wind energy capacities as of 2021 are 0.7 percent and 0.42 percent, respectively [29].

The government of the Russian Federation has therefore committed to the development of the entire RE sector. The government's target is to achieve a renewable energy share of 4.5% by 2030. The country's Energy Strategy stipulates that the percentage of RE in the energy mix must be at least 4.5% in the period from 2020–2030, producing 80–100 billion kWh/year [30,31]. However, there is a lack of detailed information on the performance of solar PV modules under Russian weather conditions for all year round. This does not help encourage individuals and private investors to use or invest in the sector. The objective of this study is to bridge this gap by assessing solar PV's technical performance and social aspect in the Sverdlovsk region of Russia. The current study predicts solar PV system's energy performance, degradation, and energy loss under different orientations, i.e., fixed tilted plane and tracking horizontal axis E–W using the PVsyst simulation software. This is the first time such a study has been conducted in the study area in the Russian Federation, to the best of our knowledge. Unlike the previously reviewed literature, this study assesses the employment potential of such systems in Russia. The results obtained in this study are expected to shape the technical and social aspects of solar PV energy in the country.

This work is organized into four sections; Section 2 covers the materials and method used for the study. The outcomes are obtainable in Section 3, the conclusion and future research recommendations are obtainable in Section 4.

2. Materials and Methods

The methodology adopted for the study, specifications of the PV modules studied, geographical information of the study area, and mathematical relations used for the evaluation of the various performance indicators are presented in this section.

2.1. PVsyst Simulation Model

The PVsyst simulation tool is a commonly used software in designing solar power plants optimally and assessing the energy yields of the plants. It uses meteorological irradiation resources, extensive knowledge of PV technology, and PV system components

for the simulation. As a result, the PVsyst tool can assist researchers and engineers to comprehend the PV system's workings to improve the system's design. The proposed grid-connected PV system was simulated using the following steps [1]:

- Identification of the study area (location)
- Downloading of the weather data characteristics for the study area (i.e., solar irradiance, wind speed, and ambient temperature)
- Selection of the orientation of the PV module (i.e., tilt and azimuth angles)
- Selection of the system components of the PV and inverter systems in relation to the requirements of the system
- Discretionary user needs relative to grid-tied system requirements
- The discretionary choice to alter the values for the loss types.

2.2. Meteorological Data of the Study Area

The study area is Yekaterinburg, which is in the Sverdlovsk region in Russia. It is located on latitude 56°50′34.4″ N and longitude 60°39′19.0″ E. The weather data used for the analysis were obtained from Meteonorm 8.0. The study area has an average global horizontal irradiation (GHI) average of 2.82 kWh/m^2/day and horizontal diffuse irradiation of 1.37 kWh/m^2/day. The average annual temperature for the area is 2.6 °C, with an average wind speed of 3.7 m/s. The relative humidity of the study area is also 74.1%, with a global horizontal irradiation year-to-year variability of 3.7%. The weather characteristics of the study area are presented in Figure 1. The lowest temperature and solar irradiation usually occur during the winter; similarly, May–August record relatively high temperatures and insolation. The month of July generally receives the highest solar irradiation and temperatures.

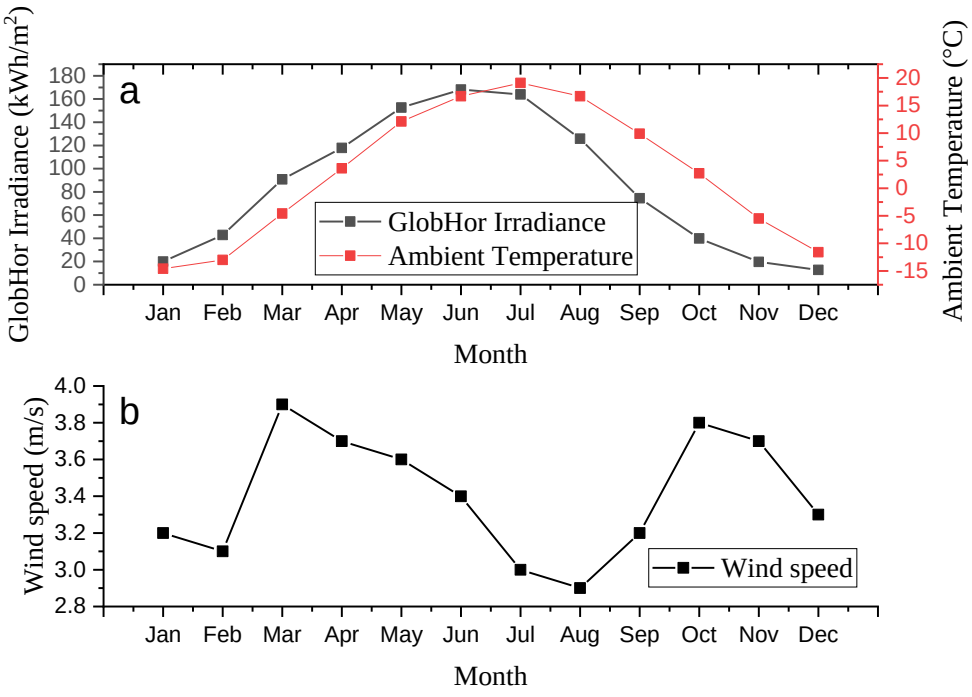

Figure 1. (**a**) GHI and temperature (**b**) wind speed characteristics of the study area (Meteonorm 8.0).

2.3. Solar PV Performance Assessment

The system yields are classified into an array, a reference, and final yields. The yields show the actual array operations in relation to its rated capacity. The array yield Y_A is said to be the output energy *DC* (direct current) produced from the *PV* array within a

certain time frame normalized by the *PV* system's rated power [32]. It can be represented mathematically as indicated in Equation (1) [33].

$$Y_A = \frac{E_{DC}}{P_{PV,\,rated}} \left(\mathrm{kWh}/\mathrm{kW_p}\right) \tag{1}$$

where E_{DC} is the *PV* array's *DC* energy output in (kWh), and $P_{PV,\,rated}$ is the *PV* system rated power in ($\mathrm{kW_p}$).

The alternating current (*AC*) energy (total) produced by the *PV* module for a specific time is divided by the installed *PV*'s system rated output power [32]. The final yield Y_F can be defined as the inverter side output, which is *AC* energy produced daily $Y_{F,\,d}$ or monthly $Y_{F,\,m}$ by the system, which is normalized by its nominal or rated power of the installed *PV* array. It can be calculated using Equation (2) [34].

$$Y_F = \frac{E_{AC}}{P_{PV,\,rated}} \tag{2}$$

where the *AC* energy output (kWh) is denoted by E_{AC}.

The reference yield Y_R describes the solar irradiance for the *PV* system; it is the total in-plane solar irradiance divided by the reference irradiance at standard test conditions (STCs). It is a function of weather conditions, array orientation, and location, as indicated in Equation (3) [9,33].

$$Y_R = \frac{G_I}{G_{STC}} \left(\mathrm{kWh/kW}\right) \tag{3}$$

where the total in-plane solar irradiance is denoted with G_I ($\mathrm{kWh/m^2}$), and the reference irradiance at STCs is represented by G_{STC} (1 $\mathrm{kW/m^2}$).

The *PR* of a solar *PV* system measures the total outcome of losses on the *PV* system's rated output. The *PV* system's *PR* shows how close its performance approaches the ideal performance under real-life operations; it helps compare a *PV* system's independence of a location, orientation, tilt angle, and nominal rated power capacity. It can be calculated using Equation (4) [32,35].

$$PR = \frac{100 \times Y_F}{Y_R} (\%) \tag{4}$$

CF can be defined as the ratio of the *AC* energy that is generated by the *PV* system within a specified period of time (mostly one year) to the system's output energy, which would have been produced if the power plant were to operate at full capacity for the entire period. The yearly *CF* can calculated using Equation (5) [6].

$$CF = \frac{E_{AC}}{P_{PV,\,rated} \times 8760} \tag{5}$$

The array capture losses L_A shows the losses occasioned by the array's operation, which highlights the array's failure to use the available irradiance [26] completely. The difference between the array yield and the reference yield is the array capture losses; this can be calculated using Equations (6) and (7) [32].

$$L_A = Y_R - Y_A \left(\mathrm{kWh/kW_p}\right) \tag{6}$$

where the losses L_S are caused by losses in changing the inverter's *DC* output power from the *PV* system to *AC* power. This is mathematically represented as follows:

$$L_S = Y_A - Y_F \left(\mathrm{kWh/kW_p}\right) \tag{7}$$

The thermal losses result from the effect of temperature on the performances of the *PV* modules. This can be expressed mathematically as indicated in Equation (8) [36].

$$E_{therm} = E_{PV}\left(1 - \frac{1}{1 - \gamma(T_C - T_0)}\right) \text{(MWh)} \quad (8)$$

where the temperature coefficient of the maximal power is denoted by γ, the module temperature under STCs (25 °C) is represented by T_0, and the module temperature is denoted by T_C.

2.4. Energy Production

The daily, monthly, and annually total energy (*AC* or *DC*) produced by the *PV* system can be attained through simple summations as shown in Equation (9) [37,38].

$$\begin{aligned} E_d &= \sum_{1}^{24} E_h \text{(kWh)} \\ E_m &= \sum_{1}^{n} E_d \text{ (kWh)} \\ E_y &= \sum_{1}^{12} E_m \text{ (kWh)} \end{aligned} \quad (9)$$

where the number of days in a month is represented by n, and the hourly energy is denoted by E_h. In addition, the daily, monthly, and yearly cumulative energy values are represented with E_d, E_m, and E_y, respectively.

2.5. Characteristics of the Various Components

The *PV* module technology used for the analysis was Si-mono. The AE 300DGM6-60 (1500) solar module manufactured by AE solar was used for the analysis. A total of 120 units were used to achieve the designed power output. The technical description of the *PV* module is presented in Table 1. Increasing the temperature of a *PV* cell decreases its output performance as a result of the increase in the rate of the internal recombination in the *PV* cell, which is caused by increased carrier concentrations. Both the electrical efficiency and the power output of the *PV* power plant relate linearly with its operating temperature. As a result, when the operating temperature of the *PV* module rises beyond 25 °C, it leads to a reduction in the semiconductor material's band-gap, which results in the reduction in the open circuit voltage [39,40]. The current-voltage (I–V) graph for the selected *PV* module for different cell temperatures is presented in Figure 2; in this graph, the negative effect of high temperatures on the performance of *PV* cells is clearly shown. The power–voltage graph, which also demonstrates the impact of solar irradiance on the output of the *PV* cell, is also represented in Figure 3.

Table 1. *PV* module system description.

Model	AE 300DGM6-60 (1500)
Module type	Si-mono
Unit nominal power	300 Wp
Nominal (*STC*)	36.0 kWp
P_{mpp}	32.3 kWp
Cell area	177 m^2
Module area	197 m^2
Efficiency	18.38%

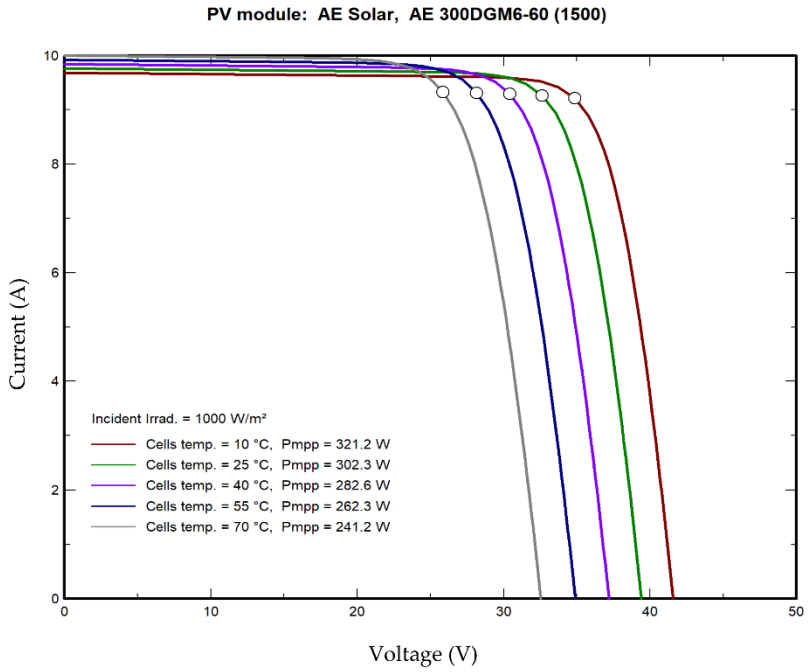

Figure 2. I-V graph for the used *PV* module under different temperature conditions (Obtained from *PV*syst software).

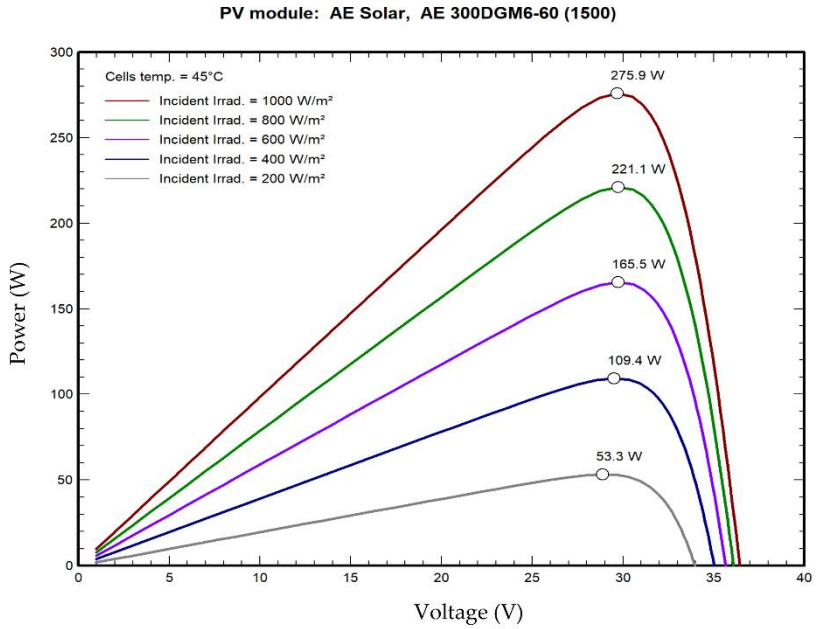

Figure 3. Power–voltage characteristics under different incident irradiance (Obtained from *PV*syst software).

In the inverter case, the Voltwerk model was used for the analysis; the model is 11 kW 400–800 V TL 50 Hz VS11 with a minimum MPP voltage of 400 V and a maximum MPP voltage of 800 V. It has a maximum efficiency of 98%. A total of 3 inverters were used to design the power plant.

Figure 4 depicts the schematic for the proposed *PV* system; it is made up of the *PV* array section where the *PV* modules are connected, the inverter section where the conversion of *DC* to *AC* is done, the load section, and the grid section. In the scheme, the E_{Array} denotes the *PV* array's energy output, while the inverter's energy output is represented by $E_{out\ inv}$. E_{used} denotes the energy used by the user load.

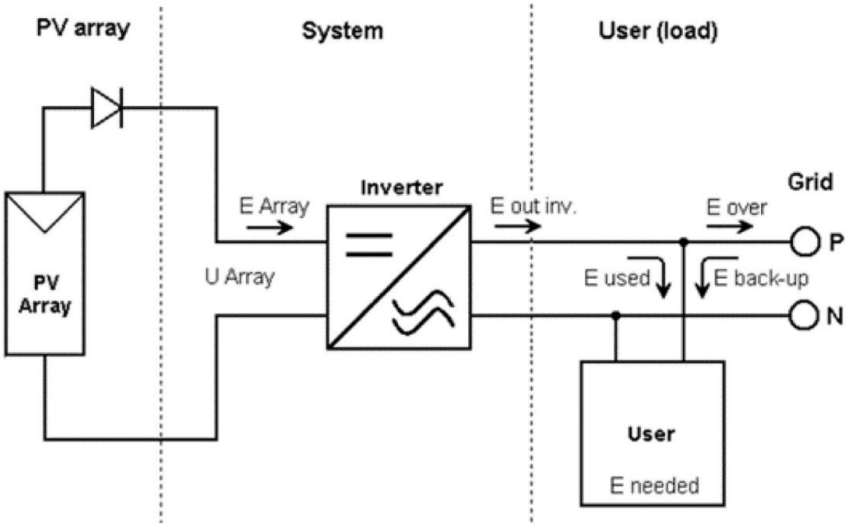

Figure 4. Schematic diagram of the proposed *PV* system.

2.6. Field Mechanisms Used in the Analysis

To take maximum advantage of the irradiation from the sun, *PV* panels are mostly tilted in the direction of the equator at an optimal tilt angle. The optimum tracking angle at a location is determined by both the latitude and the climatic conditions at the said location. There is the option to use the fixed tilted plane, which is commonly used; however, there is an option to use trackers. The single solar tracking and double-axis tracking option can be employed; this is subject to the degree of the freedom movement. The single solar tracking uses a single pivot point for rotation to track the sun's path from one point to another. In the case of the double-axis tracking, it tracks the sun's path in two different axes using two pivot points for rotation; it has both the horizontal and vertical axes [41,42]. In this study, two different field types were compared to assess their effect on the performance of the *PV* power plant at the study site. These are the fixed tilted plane and the tracking horizontal axis E–W. The optimum tilt angle for the fixed *PV* system is 45° for the study area. The two different mechanisms are represented in Figure 5.

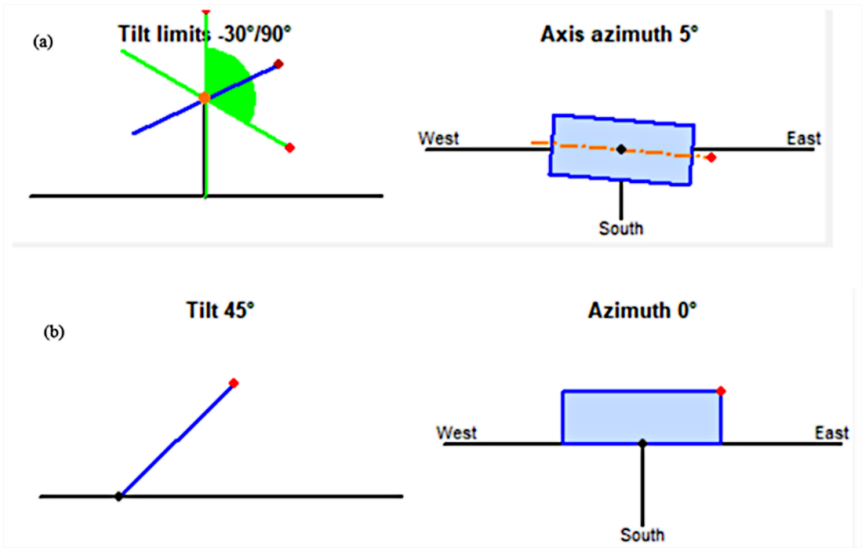

Figure 5. The orientation used, (**a**) tracking horizontal axis E–W and (**b**) fixed tilted plane.

3. Results and Discussion

According to a summary of the results from the simulations, the fixed tilted *PV* system will produce an energy of 39.5 MWh/year with an estimated specific production

of 1097 kWh/kWp/year and a *PR* of 82.3%, as shown in Figure 6. Similarly, the tracking horizontal axis E–W system will generate a total of 43.0 MWh/year, which is about 3.5 MWh/year more than that of the fixed tilted plane; it is also expected to record a specific production of 1194 kWh/kWp/year with a *PR* of 82.6%. As widely published in the literature, the performance of *PV* systems depends on several factors; some of these include the ambient temperature, clearness index, and the level of solar irradiation, among others. As reviewed in the introduction section of this work, the obtained *PR* in this study falls within the range of values obtained by studies, such as Malvoni et al. [8] under Mediterranean weather conditions, which obtained 84.4%. Eke and Demircan [43] obtained a *PR* of 72% under Turkey climatic conditions; similarly, Okello et al. [44] obtained 84.3% as the *PR* for a 3.2 kWp grid-connected *PV* system in South Africa. As presented earlier in this section, the slight differences in the *PR* values can be attributed to the factors that affect the *PV* system's performance. The high temperatures during the summer period affected the *PR* during those periods. The output performance of the *PV* decreases with an increase in *PV* temperature [39,45]. Hence the output performance of the system reduces to some level even if there is enough solar radiation. A malfunction in the *PV* system can also be detected based on the *PR* values. Months with lower *PR* can be ascribed to a malfunction in the inverter and the incorrect functioning of the system. The IEC norm describes the normalized production and represents the standardized parameter for the *PV* system's performance assessment. It can therefore be assessed to compare the characteristics of *PV* architectures that are constructed under similar climatic conditions [46]. The useful produced energy per installed kWp/day, system losses, and the collection losses for both orientations are estimated and presented in Figure 7. The arrays' temperature characteristics against effective irradiance are presented in Figure 8. It can be seen from the figure that the array's temperature ranged between −30 °C during the winter period to as high as about 65 °C in the summer period.

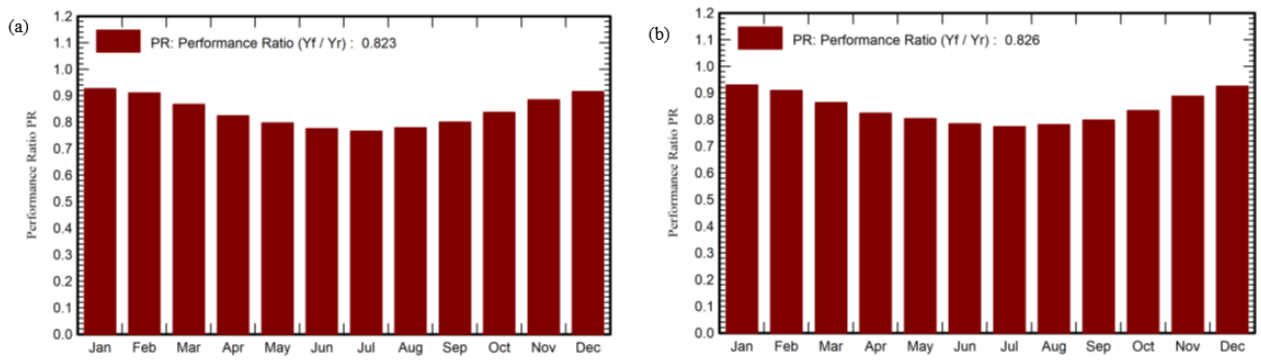

Figure 6. Monthly performance ratio for the (**a**) fixed plane and (**b**) tracking *PV* system.

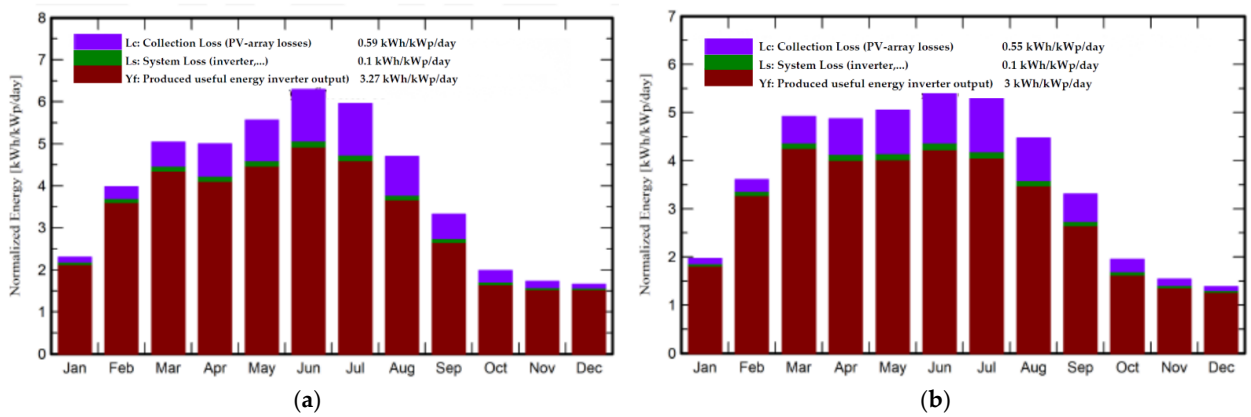

Figure 7. Normalized energy production per installed kWp for (**a**) fixed plane (**b**) tracking *PV* system.

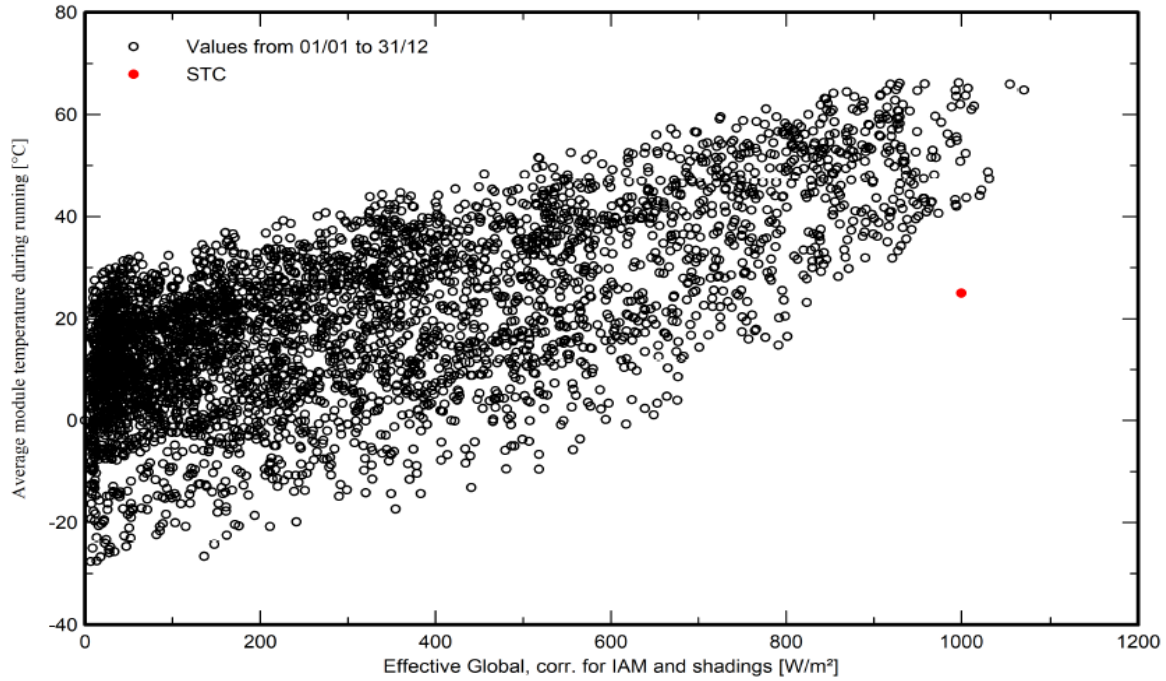

(**a**)

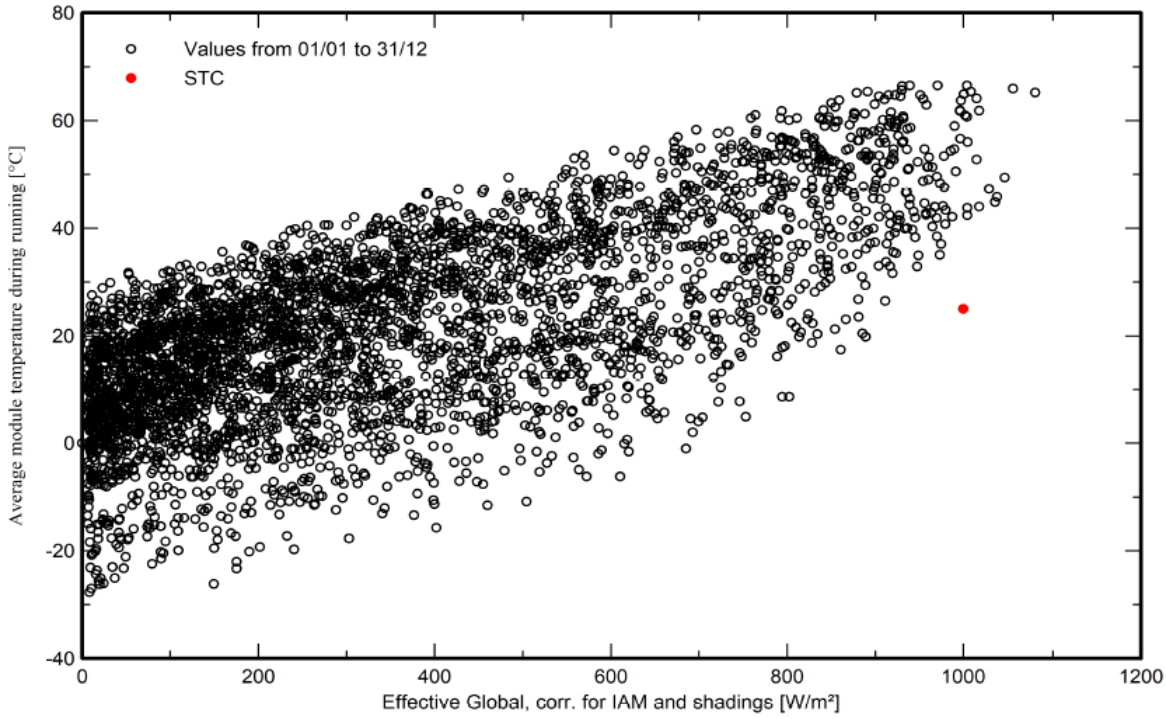

(**b**)

Figure 8. Array temperature vs. effective irradiance (**a**) fixed plane and (**b**) tracking *PV* system.

The expected monthly energy injected into the grid from the *PV* system for both orientations is shown in Figure 9. It is evident that the most energy injected into the grid occurs during the summer period, obviously because of the longer period and high intensity of solar radiation during that time. The balances and main results are presented in Table 2; it includes the global horizontal, horizontal diffuse irradiance, effective global corresponding for shading (GlobEff), ambient temperature (T_amb), global incident in collector plane (GlobInc), the energy output of the *PV* array (EArray), performance ratio

(*PR*), and the energy injected into the grid (E_Grid for each month of the year as well as the overall energy out for the year. Although the highest solar irradiation at the study area occurs during the summer periods, it is clear from the Table that the *PR* at those periods is relatively lower compared to the other periods. This may be due to the relatively high temperatures during those areas, which negatively affect the efficiency of the solar cells. It is clear from the energy values presented in Table 1 that both designs lost energy in the course of the conversion as there is a difference between the *DC* and *AC* sides of the energy produced. This difference is the energy lost due to the losses in the system. The fixed tilted plane system lost 1.249 MWh against 1.277 MW for the tracking system.

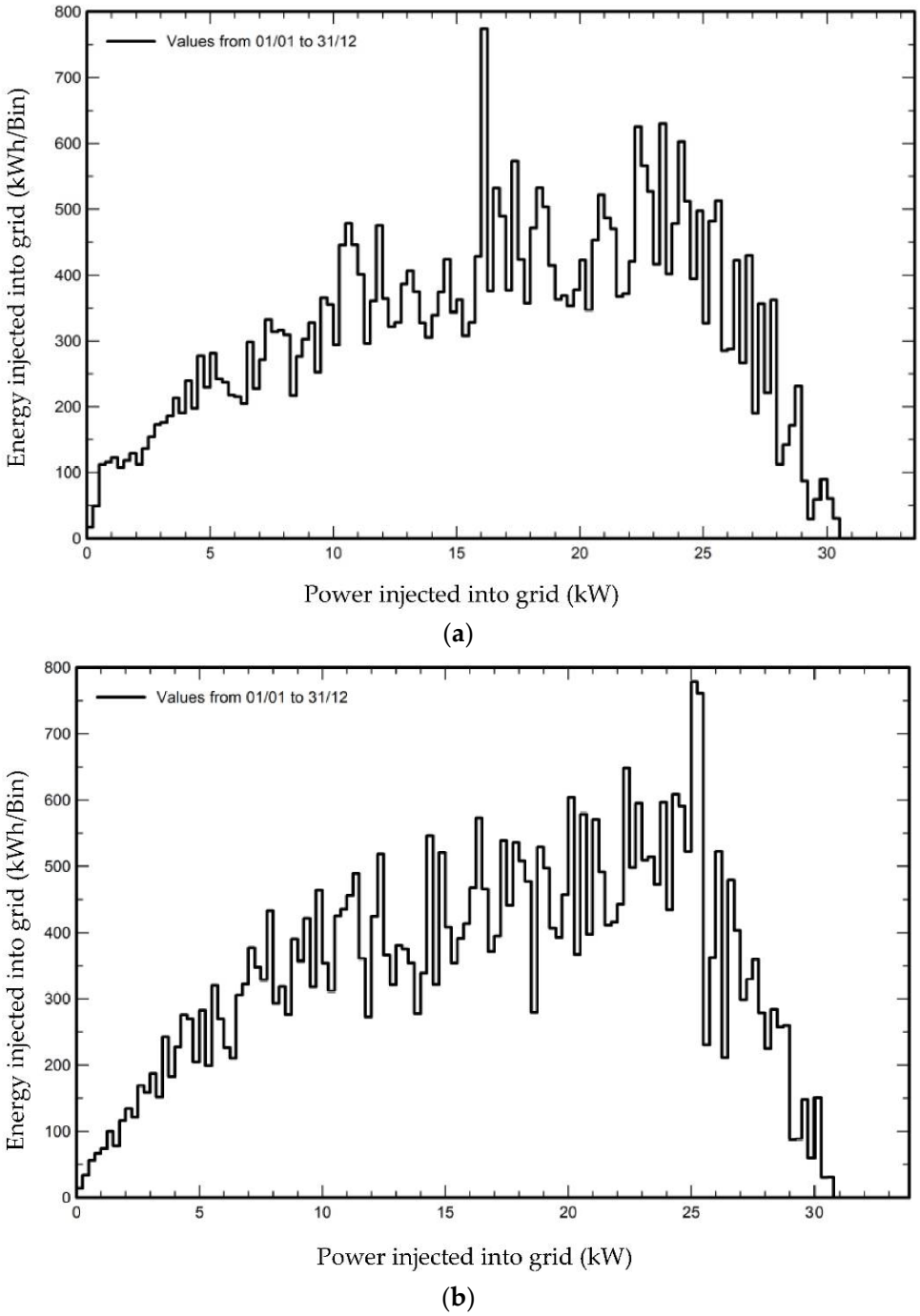

Figure 9. System output power distribution (**a**) fixed plane and (**b**) tracking system.

Table 2. Balances and main results.

	Global Horizontal, kWh/m²	Diffuse Horizontal, kWh/m²	T_amb, °C	Global Eff, kWh/m²		GlobInc, kWh/m²		Energy Array, MWh		E_Grid, MWh		*PR*	
				Fixed	Tracking	Fixed	Tracking	Fixed	Tracking	Fixed	Tracking	Tracking	Fixed
Jan	19.9	10.17	−14.57	58.0	68.5	60.9	71.3	2.087	2.446	2.032	2.384	0.929	0.926
Feb	42.8	16.23	−13.04	96.2	106.6	101.0	111.3	3.394	3.734	3.310	3.642	0.909	0.911
Mar	90.8	33.36	−4.61	144.6	148.5	152.4	156.4	4.880	4.994	4.754	4.865	0.864	0.867
Apr	117.8	52.17	3.92	137.9	141.2	146.1	149.9	4.467	4.579	4.333	4.446	0.824	0.824
May	152.6	77.64	12.05	147.5	162.6	156.4	172.6	4.634	5.136	4.489	4.991	0.803	0.797
Jun	168.1	76.44	16.66	154.5	178.0	163.9	188.6	4.725	5.481	4.576	5.329	0.785	0.776
Jul	163.9	78.29	19.14	154.9	174.1	164.3	184.7	4.680	5.291	4.531	5.140	0.773	0.766
Aug	125.8	69.21	16.66	130.7	137.1	138.6	145.6	4.014	4.222	3.885	4.093	0.781	0.779
Sep	74.5	39.26	9.94	93.8	94.3	99.3	99.8	2.965	2.974	2.862	2.870	0.799	0.801
Oct	39.8	26.93	2.66	57.3	58.4	60.5	61.4	1.896	1.920	1.821	1.844	0.834	0.837
Nov	19.7	11.85	−5.47	44.0	49.7	46.3	51.8	1.527	1.711	1.473	1.655	0.887	0.884
Dec	12.8	7.59	−11.64	40.9	49.4	43.0	51.3	1.463	1.758	1.417	1.710	0.925	0.916
Year	1028.4	499.14	2.73	1260.3	1368.5	1332.6	1444.9	40.732	44.247	39.483	42.970	0.826	0.823

The *PV*syst also runs a probability distribution analysis for the total yearly energy produced from the system, which could be transferred into the grid system. The probability distribution variance for the plant's production forecast depends on several factors; some of these include inverter efficiency uncertainty, *PV* module modeling/parameters, meteo data, degradation uncertainty, and soiling and mismatch uncertainties [12]. The probability law supposes that during the many years of operation of the *PV* system, the annual yield distribution will follow a statistical law, and this law is assumed to be the normal or Gaussian distribution. The P50-P90 indicates the different levels of yield, for which the probability that a particular year's production is over this value of 50% and 90%, respectively [47]. The probability distribution function for the *PV* plant's energy generation forecast is as shown in Figure 10. According to the results from the simulations, the expected annual production probability for the fixed *PV* module for the P50, P75, and P90 is 39.68 MWh, 37.72 MWh, and 35.94 MWh, respectively, with a variability of 2.91 MWh. In the case of the tracking *PV* module, the annual production probability for the P50, P75, and P90 is 43.18 MWh, 41.05 MWh, and 39.12 MWh, respectively, with a variability of 3.17 MWh.

3.1. System Losses

These are losses in the system that may occur during the conversion of the incident solar energy to electric energy. These losses enable users to know the energy converted into electricity by the system, which can be done by subtracting the total loss from the incident energy on the panel. The decrease in the performance of the *PV* module can be associated with these losses. The normalized production and loss factors for both orientations are presented in Figure 11. The *PV* array losses for both orientations, i.e., fixed and tracking, are 15.1% and 14.9%, respectively. The months of May to August recorded the highest array losses due to the high temperatures and relatively low wind speed during those periods. However, the tracking system positively impacted the *PV* module, as its system losses were relatively less than the fixed *PV* module. The produced useful energy (inverter output) for the fixed and tracked systems are 82.3% and 82.6%, respectively.

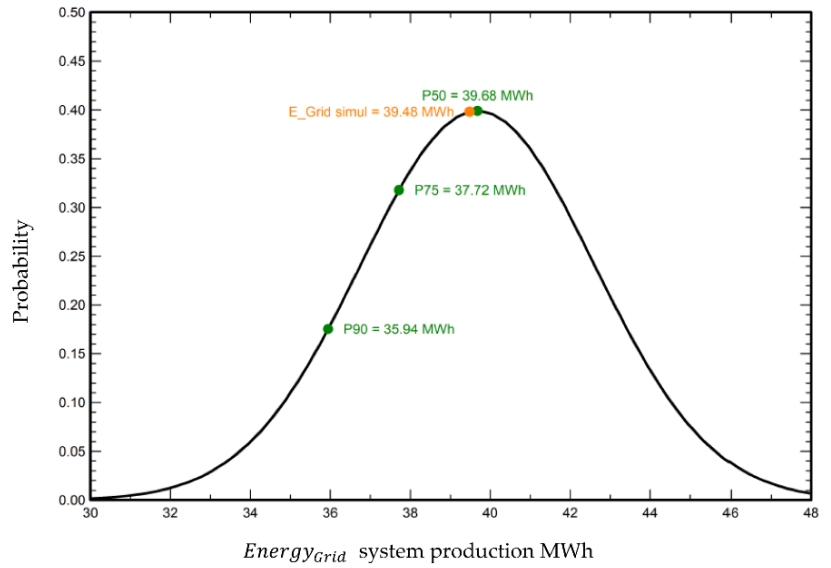

(**a**)

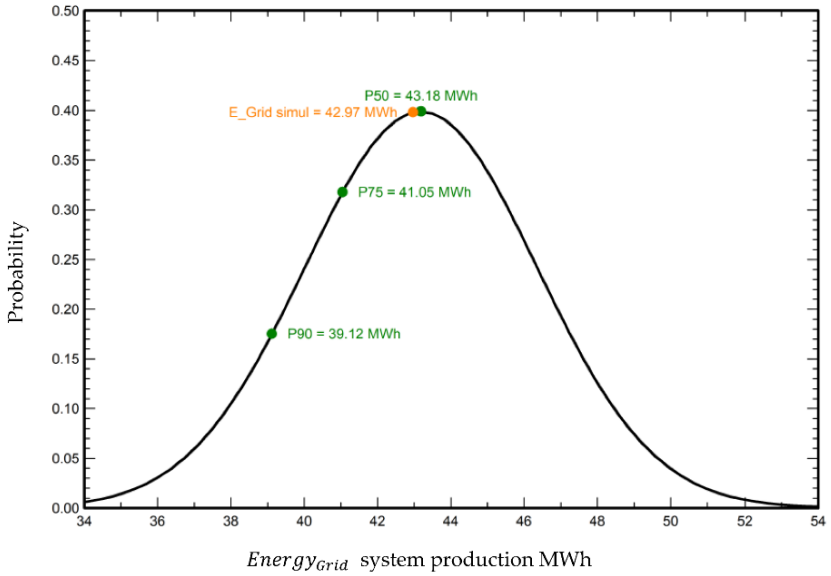

(**b**)

Figure 10. Probability distribution for (**a**) fixed and (**b**) tracking *PV* modules.

The loss diagram for the two orientations is presented in Figure 12. The losses range from the incidence angle modifier (IAM), which is the reflection loss (optical effect) that corresponds to the weakening of the irradiation that is actually reaching the surface of the *PV* cell with respect to the irradiation under normal incidence [48]. Others include manufacture losses, ambient temperature, and ohmic wiring, etc. Soiling loss involves dirt or dust accumulation on the surface of the module, which produces a dimming effect on the incident solar irradiation. The results suggest that both orientations are expected to record a soiling loss of 3%. The soiling loss can be mitigated by periodically washing the surface of the *PV* module; it can, however, add to the operations and maintenance costs, which can affect the plant's economic viability. This is especially for sites with water scarcity. The IAM loss is 2.5% for both designs. The nominal array energy (at *STC* efficiency) is 45.72 MWh for the fixed module; it, however, increased significantly by some 3.92 MWh for the tracking system.

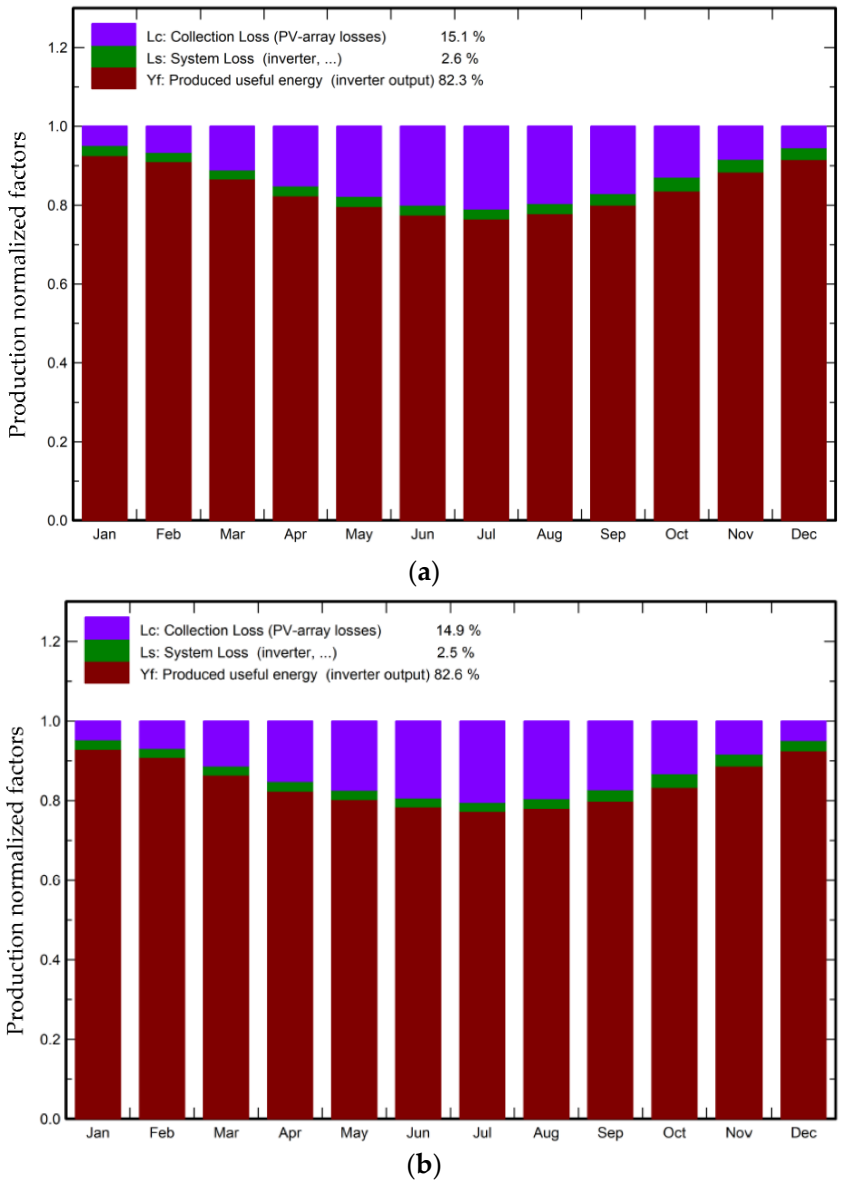

Figure 11. Normalized production and loss factors (**a**) fixed and (**b**) tracking systems.

The module quality loss, the deviation between the nominal capacity indicated on the manufacturer's datasheet, and the real module capacity, signifies the loss of module quality. A module quality loss of 0.4% was recorded. The *PV* array mismatch loss for both designs is the same; they both recorded 3.66%. This power loss is known as electrical mismatch loss. According to a study by Koirala et al. [49], a mismatch loss of up to 12% in the series string may arise but can be reduced to between 0.4–2.4% using suitable series-parallel connections. Presorting according to the max power current is identified as the most effective method for optimizing *PV* array performance [50,51]. The module degradation loss for the two designs is the same for all; they all recorded 3.82%. A total of 1028 kWh/m^2 global horizontal solar irradiation was received during the analysis period.

The two *PV* system's predicted performances were compared with other literature to assess their performance. Results from the other works on other countries presented in Table 3 can be said to be relatively similar to what is presented in this study. The *PR* falls within the range obtained by most studies.

Table 3. Comparison with other studies.

Location	Plant Capacity	Solar Irradiation (kWh/m^2)	Energy to Grid (MWh)	*PR*, %	Degradation Loss, %	Ref
India	10 MW	1940	15 798.192	86.12	-	[52]
India	186 kW	1821	318.52	85.6	-	[53]
Afghanistan	700 kW	1998	1266.1	79.7	1.50	[54]
Chile	8.2 kW	-	6.7780	85.5	-	[46]
Malaysia	380 kW	1631	495.39	80.3	3.81	[55]
India	200 kW	1820.7	292.954	77.27	2.5	[9]
Indonesia	41.1 kW	1732	74.3	82.69	-	[56]
India	230 W	1911	1.068	72.8	1.5	[57]
Vietnam	2 kW	1616	2.5699	76.9	2.0	[58]
Dubai	200 kW	2000	352.62	81.7	-	[59]
Poland	1 kW	-	0.83	60–80	-	[60]
Norway	220–240 W	-	11.92	83.03	-	[61]
Ireland	1.72 kW	1043.1	-	81.5	-	[62]
Serbia	2 kW	-	-	93.6	-	[63]
Norway	2.1 kW	-	1.93	-	-	[64]
Fixed tilted plane	36 kW	1028	39.48	82.3	3.82	Current study
Tracking system	36 kW	1028	42.97	82.6	3.82	Current study

3.2. Social Aspect

Deployment of energy systems at any location is usually accompanied by job creation, as people will be needed from the construction stages to the operation and decommissioning phase [65]. As a result, the study considered the social aspect of the energy systems to assess their employment creation potentials for the study area. The estimated employment potentials for solar *PV* is estimated to be about 0.27549 $\times$ (10^{-7}/kWh/year) [65,66]. According to the simulated results, the total energy exported to the grid per year for the fixed axis solar *PV* module is 39,480 kWh against 42,970 kWh for the tracking axis module. According to the mathematical computations, we obtained 0.0011 persons/year for the fixed *PV* module, while 0.0012 persons/year were obtained for the tracking system. Therefore, assuming both modules operated for a lifetime of 25 years, then the fixed module will have an employment potential of 0.028 persons against 0.030 persons for the tracking *PV* module. The employment potential between the two designs does not vary much. It is important to state that this analysis is only meant to assess the employment potential of the 36 kWp capacity *PV* modeled. Hence, it indicates the employment potential of a large-scale solar *PV* power plant under Russian weather conditions.

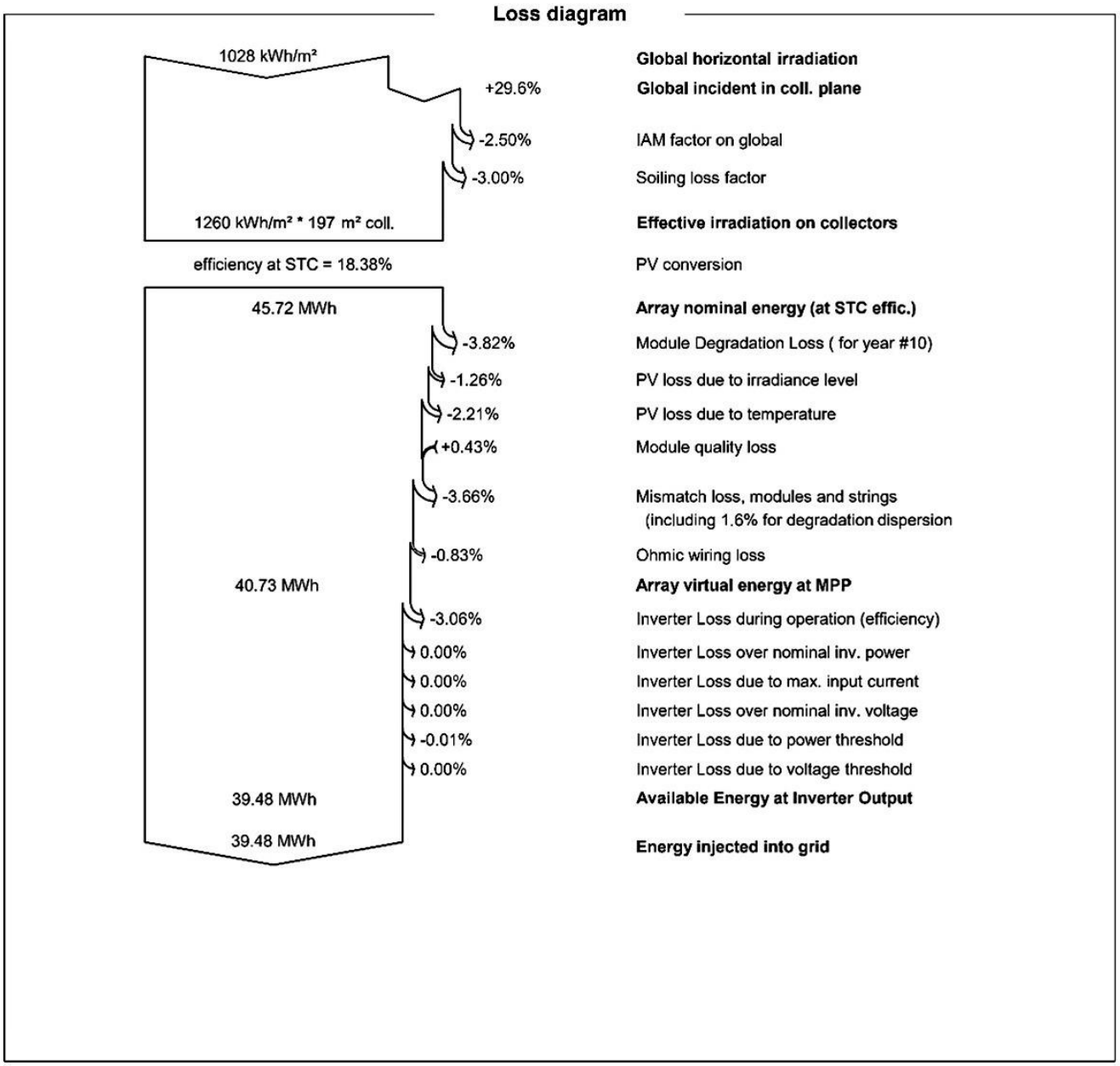

(**a**)

Figure 12. *Cont.*

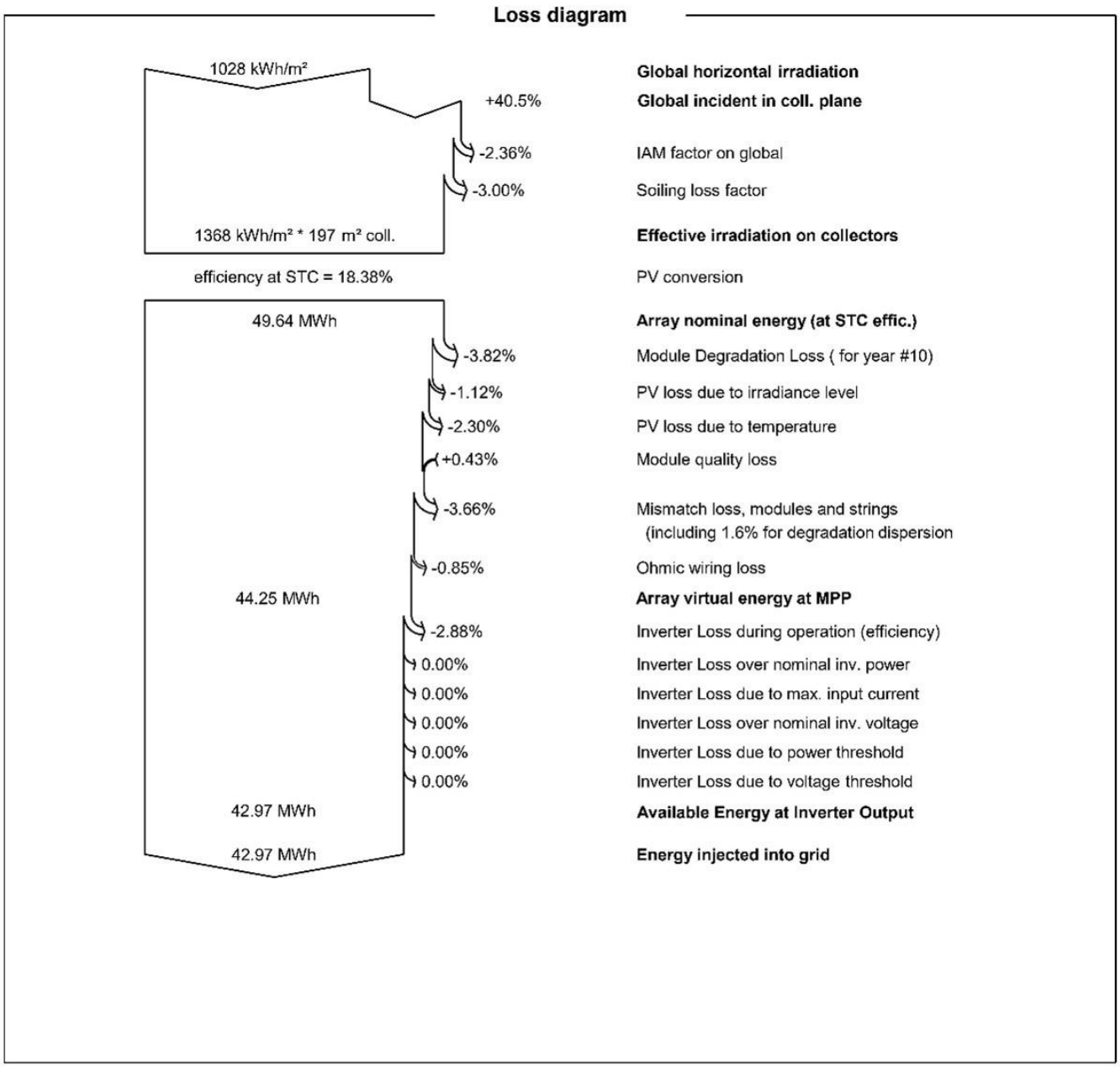

(**b**)

Figure 12. Loss diagram for (**a**) fixed and (**b**) tracking systems.

4. Conclusions

Russian weather conditions are considered harsh for large-scale solar power plants, especially due to the high negative temperatures during its long winter. Therefore, this study simulated two different designs (i.e., fixed tilted plane and tracking, horizontal axis E–W) to assess their performance, energy loss, and employment potential for potential large-scale solar *PV* development in the Sverdlovsk region of Russia. The following conclusions are made from the study:

- A total of 1028 kWh/m^2 global horizontal solar irradiation was received during the analysis period.
- The fixed tilted plane *PV* panel is expected to export 39.48 MWh of electricity to the grid, while the tracking system will export 42.97 MWh for a year. The months of March

to August are the periods within which much of the electricity will be generated due to the high solar irradiations recorded during those periods.

- A *PR* of 82.3% and 82.6% were obtained for the fixed and tracking systems, respectively. It can clearly be seen that the *PR* is inversely proportional to the temperature of the *PV* module; *PR* values in the winter season are higher than those in summer.
- According to the results from the simulations, the expected annual production probability for the fixed *PV* module for the P50, P75, and P90 is39.68 MWh, 37.72 MWh, and 35.94 MWh, respectively, with a variability of 2.91 MWh. In the case of the tracking *PV* module, the projected annual production probability for the P50, P75, and P90 is 43.18 MWh, 41.05 MWh, and 39.12 MWh, respectively, with a variability of 3.17 MWh.
- The *PV* array losses for both orientations, i.e., fixed and tracking, are expected to be 15.1% and 14.9%, respectively. The months of May to August recorded the highest array losses due to the high temperatures during those periods.
- According to the mathematical computations, we obtained 0.0011 persons/year for the fixed *PV* module, while 0.0012 persons/year were obtained for the tracking system. Therefore, assuming both modules operated for a lifetime of 25 years, then the fixed module will have an employment potential of 0.028 persons against 0.030 persons for the tracking *PV* module.

Russia is currently implementing measures that seek to promote, develop, and use its various RE resources to help cut down its GHG emissions. Therefore, this study is expected to serve as a reference material for government, interested parties, individuals, and policymakers in relation to small and large-scale solar *PV* development, using the performance of the two designs. The data provided in this study give useful information on the possible net energy output of such systems. Future studies can assess the economic viability of such projects on large-scale levels and possibly integrate them with other renewable energy resources, such as wind, to assess their viability for rural and far-to-reach areas in Russia. An environmental impact assessment can also be assessed for large-scale *PV* projects in the country to know the potential reduction in GHG emissions that such projects come with. Similarly, future studies can conduct experimental research to compare actual results and the simulated results to give a real understanding of the performance of *PV* modules under Russian weather conditions. This is because it is highly possible that the simulated results may differ from that conducted under real environmental conditions. It is also recommended to evaluate the performance of different *PV* technologies under Russian weather conditions. This would provide critical information on the optimum technology for Russian weather.

Author Contributions: Conceptualization, E.B.A.; methodology, E.B.A.; software, E.B.A.; validation, E.B.A., U.M., S.K., M.S., E.E. and T.S.A.; formal analysis, E.B.A., U.M., S.K. and T.S.A.; investigation, E.B.A.; resources, E.B.A.; data curation, E.B.A., U.M., S.K. and T.S.A.; writing—original draft preparation, E.B.A.; writing—review and editing, E.B.A., U.M., S.K., M.S. and E.E.; visualization, E.B.A., U.M. and S.K.; project administration, E.B.A., U.M., S.K.; funding acquisition, E.B.A., S.K., M.S. and E.E. All authors have read and agreed to the published version of the manuscript.

Funding: This research was funded by Taif University Researchers Supporting Project number (TURSP-2020/61), Taif University, Taif, Saudi Arabia.

Institutional Review Board Statement: Not applicable.

Informed Consent Statement: Not applicable.

Data Availability Statement: Data used, and their sources are provided in the text.

Acknowledgments: The authors would like to thank Cardiff University/School of Engineering for accepting to pay the APC toward publishing this paper. In addition, the authors would like to acknowledge the financial support received from Taif University Researchers Supporting Project Number (TURSP-2020/61), Taif University, Taif, Saudi Arabia.

Conflicts of Interest: The authors declare no conflict of interest.

Abbreviations

AC	Alternating current
CF	Capacity factor
CIS	Copper indium selenium
DC	Direct current
E–W	East to West
GHG	Greenhouse gas
GHI	Global horizontal irradiation
IAM	Incidence angle modifier
MPP	Maximum Power Point
PR	Performance ratio
STCs	Standard test conditions

References

1. Ahmed, N.; Naveed Khan, A.; Ahmed, N.; Aslam, A.; Imran, K.; Sajid, M.B.; Waqas, A. Techno-Economic Potential Assessment of Mega Scale Grid-Connected PV Power Plant in Five Climate Zones of Pakistan. *Energy Convers. Manag.* **2021**, *237*, 114097. [CrossRef]
2. Abdin, Z.; Mérida, W. Hybrid Energy Systems for Off-Grid Power Supply and Hydrogen Production Based on Renewable Energy: A Techno-Economic Analysis. *Energy Convers. Manag.* **2019**, *196*, 1068–1079. [CrossRef]
3. IPCC. Global Warming of 1.5 °C. 2018. Available online: https://www.ipcc.ch/sr15/download/ (accessed on 2 December 2021).
4. Yaqoob, S.J.; Motahhir, S.; Agyekum, E.B. A New Model for a Photovoltaic Panel Using Proteus Software Tool under Arbitrary Environmental Conditions. *J. Clean. Prod.* **2022**, *333*, 130074. [CrossRef]
5. Agyekum, E.B.; Nutakor, C.; Agwa, A.M.; Kamel, S. A Critical Review of Renewable Hydrogen Production Methods: Factors Affecting Their Scale-Up and Its Role in Future Energy Generation. *Membranes* **2022**, *12*, 173. [CrossRef]
6. Agyekum, E.B. Techno-Economic Comparative Analysis of Solar Photovoltaic Power Systems with and without Storage Systems in Three Different Climatic Regions, Ghana. *Sustain. Energy Technol. Assess.* **2021**, *43*, 100906. [CrossRef]
7. Hassan, Q.; Jaszczur, M.; Przenzak, E. Mathematical Model for the Power Generation from Arbitrarily Oriented Photovoltaic Panel. *E3S Web Conf.* **2017**, *14*, 01028. [CrossRef]
8. Malvoni, M.; Leggieri, A.; Maggiotto, G.; Congedo, P.M.; De Giorgi, M.G. Long Term Performance, Losses and Efficiency Analysis of a 960kWp Photovoltaic System in the Mediterranean Climate. *Energy Convers. Manag.* **2017**, *145*, 169–181. [CrossRef]
9. Kumar, N.M.; Gupta, R.P.; Mathew, M.; Jayakumar, A.; Singh, N.K. Performance, Energy Loss, and Degradation Prediction of Roof-Integrated Crystalline Solar PV System Installed in Northern India. *Case Stud. Therm. Eng.* **2019**, *13*, 100409. [CrossRef]
10. Ramanan, P.; Kalidasa, M.K.; Karthick, A. Performance Analysis and Energy Metrics of Grid-Connected Photovoltaic Systems. *Energy Sustain. Dev.* **2019**, *52*, 104–115. [CrossRef]
11. Ameur, A.; Sekkat, A.; Loudiyi, K.; Aggour, M. Performance Evaluation of Different Photovoltaic Technologies in the Region of Ifrane, Morocco. *Energy Sustain. Dev.* **2019**, *52*, 96–103. [CrossRef]
12. Dahmoun, M.E.-H.; Bekkouche, B.; Sudhakar, K.; Guezgouz, M.; Chenafi, A.; Chaouch, A. Performance Evaluation and Analysis of Grid-Tied Large Scale PV Plant in Algeria. *Energy Sustain. Dev.* **2021**, *61*, 181–195. [CrossRef]
13. Kittner, N.; Gheewala, S.H.; Kamens, R.M. An Environmental Life Cycle Comparison of Single-Crystalline and Amorphous-Silicon Thin-Film Photovoltaic Systems in Thailand. *Energy Sustain. Dev.* **2013**, *17*, 605–614. [CrossRef]
14. Padmavathi, K.; Daniel, S.A. Performance Analysis of a 3MWp Grid Connected Solar Photovoltaic Power Plant in India. *Energy Sustain. Dev.* **2013**, *17*, 615–625. [CrossRef]
15. Radue, C.; van Dyk, E.E. A Comparison of Degradation in Three Amorphous Silicon PV Module Technologies. *Sol. Energy Mater. Sol. Cells* **2010**, *94*, 617–622. [CrossRef]
16. Kymakis, E.; Kalykakis, S.; Papazoglou, T.M. Performance Analysis of a Grid Connected Photovoltaic Park on the Island of Crete. *Energy Convers. Manag.* **2009**, *50*, 433–438. [CrossRef]
17. Belmahdi, B.; Bouardi, A.E. Solar Potential Assessment Using PVsyst Software in the Northern Zone of Morocco. *Procedia Manuf.* **2020**, *46*, 738–745. [CrossRef]
18. Kapoor, S.; Sharma, A.K.; Porwal, D. Design and Simulation of 60kWp Solar On-Grid System for Rural Area in Uttar-Pradesh by "PVsyst". *J. Phys. Conf. Ser.* **2021**, *2070*, 012147. [CrossRef]
19. Dellosa, J.T.; Panes, M.J.C.; Espina, R.U. Techno-Economic Analysis of a 5 MWp Solar Photovoltaic System in the Philippines. In Proceedings of the 2021 IEEE International Conference on Environment and Electrical Engineering and 2021 IEEE Industrial and Commercial Power Systems Europe (EEEIC/I CPS Europe), Bari, Italy, 7–10 September 2021; pp. 1–6.
20. Chabachi, S.; Necaibia, A.; Abdelkhalek, O.; Bouraiou, A.; Ziane, A.; Hamouda, M. Performance Analysis of an Experimental and Simulated Grid Connected Photovoltaic System in Southwest Algeria. *Int. J. Energy Environ. Eng.* **2022**. [CrossRef]
21. Yadav, B.K.; Rauniyar, P.K.; Sudhakar, K.; Bajracharya, T.R.; Priya, S.S. Sustainable Green Campus in NEPAL: 3E Analysis. *Int. J. Low-Carbon Technol.* **2021**, *16*, 531–542. [CrossRef]

22. Haffaf, A.; Lakdja, F.; Ould Abdeslam, D.; Meziane, R. Monitoring, Measured and Simulated Performance Analysis of a 2.4 KWp Grid-Connected PV System Installed on the Mulhouse Campus, France. *Energy Sustain. Dev.* **2021**, *62*, 44–55. [CrossRef]
23. Chandel, R.; Chandel, S.S. Performance Analysis Outcome of a 19-MWp Commercial Solar Photovoltaic Plant with Fixed-Tilt, Adjustable-Tilt, and Solar Tracking Configurations. *Prog. Photovolt. Res. Appl.* **2022**, *30*, 27–48. [CrossRef]
24. Kumar, P.; Pal, N.; Sharma, H. Performance Analysis and Evaluation of 10 KWp Solar Photovoltaic Array for Remote Islands of Andaman and Nicobar. *Sustain. Energy Technol. Assess.* **2020**, *42*, 100889. [CrossRef]
25. Korsavi, S.S.; Zomorodian, Z.S.; Tahsildoost, M. Energy and Economic Performance of Rooftop PV Panels in the Hot and Dry Climate of Iran. *J. Clean. Prod.* **2018**, *174*, 1204–1214. [CrossRef]
26. Omar, M.A.; Mahmoud, M.M. Grid Connected PV- Home Systems in Palestine: A Review on Technical Performance, Effects and Economic Feasibility. *Renew. Sustain. Energy Rev.* **2018**, *82*, 2490–2497. [CrossRef]
27. Elibol, E.; Özmen, Ö.T.; Tutkun, N.; Köysal, O. Outdoor Performance Analysis of Different PV Panel Types. *Renew. Sustain. Energy Rev.* **2017**, *67*, 651–661. [CrossRef]
28. Agyekum, E.B.; Kumar, N.M.; Mehmood, U.; Panjwani, M.K.; Haes Alhelou, H.; Adebayo, T.S.; Al-Hinai, A. Decarbonize Russia—A Best–Worst Method Approach for Assessing the Renewable Energy Potentials, Opportunities and Challenges. *Energy Rep.* **2021**, *7*, 4498–4515. [CrossRef]
29. Statista. Russia: Installed Electricity Generation Capacity by Source. 2021. Available online: https://www.statista.com/statistics/1027465/russia-installed-electricity-generating-capacity-by-source/ (accessed on 27 January 2022).
30. IRENA. *REMAP 2030 Renewable Energy Prospects for the Russian Federation*; IRENA: Abu Dhabi, United Arab Emirates, 2017; Available online: www.irena.org/remap (accessed on 15 December 2021).
31. Institute of Energy Strategy. *Energy Strategy of Russia for the Period Up to 2030*; Institute of Energy Strategy: Moscow, Russia, 2010; p. 174.
32. de Lima, L.C.; de Araújo Ferreira, L.; de Lima Morais, F.H.B. Performance Analysis of a Grid Connected Photovoltaic System in Northeastern Brazil. *Energy Sustain. Dev.* **2017**, *37*, 79–85. [CrossRef]
33. Chandrika, V.; Thalib, M.M.; Karthick, A.; Sathyamurthy, R.; Manokar, A.M.; Subramaniam, U.; Stalin, B. Performance Assessment of Free Standing and Building Integrated Grid Connected Photovoltaic System for Southern Part of India. *Build. Serv. Eng. Res. Technol.* **2021**, *42*, 237–248. [CrossRef]
34. Ramanan, P.; Kalidasa Murugavel, K.; Karthick, A.; Sudhakar, K. Performance Evaluation of Building-Integrated Photovoltaic Systems for Residential Buildings in Southern India. *Build. Serv. Eng. Res. Technol.* **2020**, *41*, 492–506. [CrossRef]
35. Oliveira-Pinto, S.; Stokkermans, J. Assessment of the Potential of Different Floating Solar Technologies—Overview and Analysis of Different Case Studies. *Energy Convers. Manag.* **2020**, *211*, 112747. [CrossRef]
36. Elhadj Sidi, C.E.B.; Ndiaye, M.L.; El Bah, M.; Mbodji, A.; Ndiaye, A.; Ndiaye, P.A. Performance Analysis of the First Large-Scale (15MWp) Grid-Connected Photovoltaic Plant in Mauritania. *Energy Convers. Manag.* **2016**, *119*, 411–421. [CrossRef]
37. Li, C. Comparative Performance Analysis of Grid-Connected PV Power Systems with Different PV Technologies in the Hot Summer and Cold Winter Zone. *Int. J. Photoenergy* **2018**, *2018*, 8307563. [CrossRef]
38. AL-Rasheedi, M.; Gueymard, C.A.; Al-Khayat, M.; Ismail, A.; Lee, J.A.; Al-Duaj, H. Performance Evaluation of a Utility-Scale Dual-Technology Photovoltaic Power Plant at the Shagaya Renewable Energy Park in Kuwait. *Renew. Sustain. Energy Rev.* **2020**, *133*, 110139. [CrossRef]
39. Agyekum, E.B.; PraveenKumar, S.; Alwan, N.T.; Velkin, V.I.; Shcheklein, S.E. Effect of Dual Surface Cooling of Solar Photovoltaic Panel on the Efficiency of the Module: Experimental Investigation. *Heliyon* **2021**, *7*, e07920. [CrossRef] [PubMed]
40. Dubey, S.; Sarvaiya, J.N.; Seshadri, B. Temperature Dependent Photovoltaic (PV) Efficiency and Its Effect on PV Production in the World—A Review. *Energy Procedia* **2013**, *33*, 311–321. [CrossRef]
41. Agyekum, E.B.; Afornu, B.K.; Ansah, M.N.S. Effect of Solar Tracking on the Economic Viability of a Large-Scale PV Power Plant. *Environ. Clim. Technol.* **2020**, *24*, 55–65. [CrossRef]
42. Hafez, A.Z.; Yousef, A.M.; Harag, N.M. Solar Tracking Systems: Technologies and Trackers Drive Types–A Review. *Renew. Sustain. Energy Rev.* **2018**, *91*, 754–782. [CrossRef]
43. Eke, R.; Demircan, H. Performance Analysis of a Multi Crystalline Si Photovoltaic Module under Mugla Climatic Conditions in Turkey. *Energy Convers. Manag.* **2013**, *65*, 580–586. [CrossRef]
44. Okello, D.; van Dyk, E.E.; Vorster, F.J. Analysis of Measured and Simulated Performance Data of a 3.2kWp Grid-Connected PV System in Port Elizabeth, South Africa. *Energy Convers. Manag.* **2015**, *100*, 10–15. [CrossRef]
45. Agyekum, E.B.; PraveenKumar, S.; Alwan, N.T.; Velkin, V.I.; Shcheklein, S.E.; Yaqoob, S.J. Experimental Investigation of the Effect of a Combination of Active and Passive Cooling Mechanism on the Thermal Characteristics and Efficiency of Solar PV Module. *Inventions* **2021**, *6*, 63. [CrossRef]
46. Vidal, H.; Rivera, M.; Wheeler, P.; Vicencio, N. The Analysis Performance of a Grid-Connected 8.2 KWp Photovoltaic System in the Patagonia Region. *Sustainability* **2020**, *12*, 9227. [CrossRef]
47. PVsyst Project Design > P50–P90 Evaluations. Available online: https://www.pvsyst.com/help/p50_p90evaluations.htm (accessed on 31 December 2021).
48. PVsyst Project Design > Array and System Losses > Array Losses, General Considerations. Available online: https://www.pvsyst.com/help/array_losses_general.htm (accessed on 1 January 2022).

49. Koirala, B.P.; Sahan, B.; Henze, N. Study on MPP Mismatch Losses in Photovoltaic Applications. In Proceedings of the European Photovoltaic Solar Energy Conference and Exhibition (EU PVSEC), Hamburg, Germany, 21–25 September 2009; pp. 3727–3733.
50. Tapia, M. *Evaluation of Performance Models against Actual Performance of Grid Connected PV Systems*; Carl von Ossietzky Universität Oldenburg, Institute of Physics: Oldenburg, Germany, 2013. Available online: http://oops.uni-oldenburg.de/2433/7/Thesis_TapiaM.pdf (accessed on 2 January 2022).
51. Herrmann, W.; Kämmer, S.; Yusufoglu, U. Circuit Losses in PV Arrays Caused by Electrical Mismatch of PV Modules—Impacts of Temperature Gradients and a Variation of Irradiance. In Proceedings of the 28th European Photovoltaic Solar Energy Conference and Exhibition, Villepinte, France, 30 September–4 October 2013; pp. 4127–4131.
52. Shiva Kumar, B.; Sudhakar, K. Performance Evaluation of 10 MW Grid Connected Solar Photovoltaic Power Plant in India. *Energy Rep.* **2015**, *1*, 184–192. [CrossRef]
53. Arora, R.; Arora, R.; Sridhara, S.N. Performance Assessment of 186 KWp Grid Interactive Solar Photovoltaic Plant in Northern India. *Int. J. Ambient. Energy* **2019**, *43*, 128–141. [CrossRef]
54. Baqir, M.; Channi, H.K. Analysis and Design of Solar PV System Using Pvsyst Software. *Mater. Today Proc.* **2022**, *48*, 1332–1338. [CrossRef]
55. Husain, A.A.F.; Phesal, M.H.A.; Ab Kadir, M.Z.A.; Ungku Amirulddin, U.A. Techno-Economic Analysis of Commercial Size Grid-Connected Rooftop Solar PV Systems in Malaysia under the NEM 3.0 Scheme. *Appl. Sci.* **2021**, *11*, 10118. [CrossRef]
56. Syahindra, K.D.; Ma'arif, S.; Widayat, A.A.; Fauzi, A.F.; Setiawan, E.A. Solar PV System Performance Ratio Evaluation for Electric Vehicles Charging Stations in Transit Oriented Development (TOD) Areas. *E3S Web Conf.* **2021**, *231*, 02002. [CrossRef]
57. Kumar, R.; Rajoria, C.S.; Sharma, A.; Suhag, S. Design and Simulation of Standalone Solar PV System Using PVsyst Software: A Case Study. *Mater. Today Proc.* **2021**, *46*, 5322–5328. [CrossRef]
58. Duong, M.Q.; Tran, N.T.N.; Sava, G.N.; Tanasiev, V. Design, Performance and Economic Efficiency Analysis of the Photovoltaic Rooftop System. *Rev. Roum. Sci. Tech. Électrotech. Énerg.* **2019**, *64*, 229–234.
59. Satish, M.; Santhosh, S.; Yadav, A. Simulation of a Dubai Based 200 KW Power Plant Using PVsyst Software. In Proceedings of the 2020 7th International Conference on Signal Processing and Integrated Networks (SPIN), Noida, India, 27–28 February 2020; pp. 824–827.
60. Pietruszko, S.M.; Gradzki, M. Performance of a Grid Connected Small PV System in Poland. *Appl. Energy* **2003**, *74*, 177–184. [CrossRef]
61. Adaramola, M.S.; Vågnes, E.E.T. Preliminary Assessment of a Small-Scale Rooftop PV-Grid Tied in Norwegian Climatic Conditions. *Energy Convers. Manag.* **2015**, *90*, 458–465. [CrossRef]
62. Ayompe, L.M.; Duffy, A.; McCormack, S.J.; Conlon, M. Measured Performance of a 1.72 kW Rooftop Grid Connected Photovoltaic System in Ireland. *Energy Convers. Manag.* **2011**, *52*, 816–825. [CrossRef]
63. Milosavljević, D.D.; Pavlović, T.M.; Piršl, D.S. Performance Analysis of A Grid-Connected Solar PV Plant in Niš, Republic of Serbia. *Renew. Sustain. Energy Rev.* **2015**, *44*, 423–435. [CrossRef]
64. Adaramola, M.S. Techno-Economic Analysis of a 2.1kW Rooftop Photovoltaic-Grid-Tied System Based on Actual Performance. *Energy Convers. Manag.* **2015**, *101*, 85–93. [CrossRef]
65. Chauhan, A.; Saini, R.P. Techno-Economic Feasibility Study on Integrated Renewable Energy System for an Isolated Community of India. *Renew. Sustain. Energy Rev.* **2016**, *59*, 388–405. [CrossRef]
66. Baruah, A.; Basu, M.; Amuley, D. Modeling of an Autonomous Hybrid Renewable Energy System for Electrification of a Township: A Case Study for Sikkim, India. *Renew. Sustain. Energy Rev.* **2021**, *135*, 110158. [CrossRef]